Three-dimensional structural vibration analysis by the Dual Reciprocity BEM

John Agnantiaris, Demosthenes Polyzos, Dimitri Beskos

Three-dimensional structural vibration analysis by the Dual Reciprocity BEM

J. P. Agnantiaris, D. Polyzos, D. E. Beskos

Abstract The dual reciprocity boundary element method (DR/BEM) is employed for the analysis of free and forced vibrations of three-dimensional elastic solids. Use of the elastostatic fundamental solution in the integral formulation of elastodynamics creates an inertial volume integral in addition to the boundary ones. This volume integral is transformed into a surface integral by invoking the reciprocal theorem. A general analytical method is described for the closed form determination of the particular solutions of the displacement and traction tensors corresponding to any radial basis function employed in the transformation process. The simple but effective $1 + r$ radial basis function is used in the applications of this paper. Quadratic continuous and discontinuous 9-noded boundary elements are used in the analysis. Free vibrations are studied by solving the corresponding eigenvalue problem iteratively. Harmonic forced vibration problems are solved directly in the frequency domain. Transient forced vibration problems are solved by integrating the equations of motion stepwise with the aid of various algorithms. Interior collection points are also used for assessing the accuracy of the method. Two numerical examples involving free and forced vibrations of a sphere and a cube are presented in detail.

1 Introduction

The conventional Boundary Element Method (BEM) as applied to elastodynamic analysis in the frequency or time domain employs the corresponding elastodynamic fundamental solution and formulates the problem in terms of only surface integrals, thereby reducing the dimensionality of the problem by one and restricting the discretization to the surface of the domain (Beskos 1987, 1996). However, the use of the elastodynamic fundamental solution increases the computational effort in forced vibration analysis and in addition creates problems of accuracy in free vibration analysis, due to its complicated form. On the other hand, use of the much simpler elastostatic fundamental solution creates an inertial volume integral, which requires an interior discretization of the domain in addition to the surface one. Thus, the main advantage of dimensionality reduction of the method is lost (Beskos 1987, 1996).

Nardini and Brebbia (1982, 1983, 1985) introduced the Dual Reciprocity Boundary Element Method (DR/BEM), in which the inertial volume integral is transformed into a surface integral with the aid of the reciprocal theorem applied for the second time, the first time being when formulating the elastodynamic problem in integral form. Thus, they succeeded in creating a BEM which combines the dimensionality reduction advantage with the simple elastostatic fundamental solution with obvious computational gains in both free and forced elastic vibration problems. Looking at the result from another viewpoint, one can say that the resulting formulation looks like a finite element one without the need of interior discretization but with the employment of nonsymmetric matrices. Thus, in DR/BEM, free vibration analysis is accomplished by solving the generalized eigenvalue problem iteratively and forced vibration analysis by integrating stepwise the equations of motion. Problems arising in free vibration analysis (use of the inefficient determinant search method) and forced vibration analysis (observing causality at every time step) by the conventional time domain BEM are now eliminated. The equivalence of the DR/BEM to the particular integrals BEM approach of Ahmad and Banerjee (1986) was recently established by Polyzos et al. (1994). A comprehensive literature review on the DR/BEM as applied to elastodynamics can be found in the general review article of Beskos (1996). The problem of convergence of the DR/BEM and the associated problems of selecting the best basis (or approximating) functions and including or not internal collocation points have received considerable attention in recent years. In elastodynamics one can mention the works of Chirino et al. (1994), Providakis et al. (1994) and Agnantiaris et al. (1996). Through comparison studies dealing with two-dimensional (2-D) elastodynamic fracture mechanics problems, Chirino et al. (1994) have concluded that a) a reasonable number of interior collocation points increase the accuracy of the method and b) the DR/BEM requires less computer time than either the time or frequency domain conventional BEM's. Very recent studies on the DR/BEM as applied to various 2-D elastodynamic problems by Agnantiaris et al. (1996) have revealed that a) radial basis

J. P. Agnantiaris, D. Polyzos
Department of Mechanical and Aerospace Engineering, University of Patras, GR-26500 Patras, Greece

D. E. Beskos
Department of Civil Engineering, University of Patras, GR-26500 Patras, Greece

functions not only lead to convergent solutions but due to their simplicity, permit an easy analytic computation of particular solutions, b) the simplest polynomial $1 + r$ provides the best results and c) some internal collocation points improve the accuracy of the solution.

The present paper deals with the application of the DR/BEM to three-dimensional (3-D) elastodynamic analysis including both free and forced vibration problems. Convergence of the method as affected by the number of boundary elements, the number of internal collocation points, the size of the time step and various step-by-step integration algorithms is studied through numerical examples. A general analytical method is described for the closed form determination of the particular solutions of the displacement and traction tensors corresponding to radial basis functions. The simple but effective $1 + r$ radial basis function is adopted. Quadratic continuous and discontinuous 9-noded boundary elements are used in the analysis. Free vibrations are studied by solving the corresponding eigenvalue problem iteratively. Harmonic forced vibration problems are solved directly in the frequency domain and transient forced vibration problems are solved by step-by-step integration of the equations of motion. Two numerical examples involving free and forced vibrations of a sphere and a cube are presented. Thus, the present paper can be thought of as an extension and generalization of the previous work of the authors (Agnantiaris et al. 1996) with respect to dimensionality, internal collocation point effect and numerical integration. The DR/BEM has been successfully applied by Wang and Banerjee (1988, 1990) and Wilson et al. (1990) to free vibrations of 3-D and axisymmetric structures. However, no application of the DR/BEM to forced vibrations of three-dimensional (3-D) elastic structures and no extensive convergence studies of the method have as yet appeared in the literature. The present paper consists of five sections with the first one being the present section (introduction). The second section briefly presents the DR/BEM as applied to elastodynamics. The third section describes a general analytical method for determining particular solutions. Section four deals with the numerical examples and section five presents the conclusions coming out of the present work.

2
The DR/BEM in elastodynamics

A brief review of the DR/BEM as applied to elastodynamics is presented in this section for reasons of completeness. More details can be found elsewhere (Dominguez 1993). Consider the motion of a linearly elastic body of volume Ω and surface Γ described by the governing partial differential equation

$$\mathbf{L}_x\mathbf{u}(\mathbf{x},t) = (\mathbf{L}^1_{\mathbf{x}} + \mathbf{L}^2_{\mathbf{x}})\mathbf{u}(\mathbf{x},t) = \mathbf{0} \ , \tag{1}$$

where $\mathbf{u}(\mathbf{x},t)$ is the displacement vector at point $\mathbf{x}$ and time t and the linear elastostatics operator $\mathbf{L}^1_{\mathbf{x}}$ and inertial operator $\mathbf{L}^2_{\mathbf{x}}$ are given by

$$\mathbf{L}^1_{\mathbf{x}} = \mu\mathbf{I}\Delta_{\mathbf{x}} + (\lambda+\mu)\nabla_{\mathbf{x}}\nabla_{\mathbf{x}} \ , \tag{2}$$

$$\mathbf{L}^2_{\mathbf{x}} = -\rho\mathbf{I}\frac{\partial^2}{\partial t^2} \ , \tag{3}$$

with λ and μ being the Lame elastic constants, ρ the mass density, $\mathbf{I}$ the identity tensor, Δ the Laplacian and ∇ the gradient operator. Assuming zero body forces and initial conditions one can obtain an integral representation of the solution of Eq. (1) in the form

$$\mathbf{c}(\mathbf{x})\mathbf{u}(\mathbf{x},t) = \int_\Gamma [\mathbf{u}^*(\mathbf{x},\xi)\mathbf{p}(\xi,t) - \mathbf{p}^*(\mathbf{x},\xi)\mathbf{u}(\xi,t)]\,\mathrm{d}\Gamma(\xi) - \int_{\mathbf{\Omega}} \mathbf{u}^*(\mathbf{x},\xi)\rho\ddot{\mathbf{u}}(\xi,t)\mathrm{d}\Omega(\xi) \tag{4}$$

where $\mathbf{u}^*(\mathbf{x},\xi)$ is the fundamental displacement tensor and $\mathbf{p}^*(\mathbf{x},\xi)$ the corresponding fundamental traction tensor for the elastostatic operator $\mathbf{L}^1_{\mathbf{x}}$ (Kelvin's solution), $\mathbf{p}(\xi,t)$ is the traction vector at point ξ and time t, overdots indicate differentiation with respect to time and the tensor $\mathbf{c}(\mathbf{x})$ receives the value of $\mathbf{I}$ for $\mathbf{x}\in\Omega$, $\mathbf{0}$ for $\mathbf{x}\in\Omega^c$, (1/2)$\mathbf{I}$ for $\mathbf{x}\in\Gamma$ and being smooth and is given as a function of the local geometry at $\mathbf{x}$ for $\mathbf{x}\in\Gamma$ and being nonsmooth.

Integral representation (4) has the advantage of employing the much simpler elastostatic fundamental solution pair and hence avoiding the time convolutions present in a conventional time domain BEM. However, the presence of the inertial volume integral in (4) indicates that an interior domain discretization in addition to the boundary one is necessary. Nardini and Brebbia (1982, 1983, 1985) were able to transform this volume integral into a boundary one, thereby creating an all-boundary integral formulation involving the advantageous elastostatic fundamental solution and leading to the DR/BEM. To this end, the unknown solution $\mathbf{u}(\mathbf{x},t)$ is expressed inside Ω as a series of unknown time dependent coefficients $\alpha^m_i(t)$ and known basis functions $f^m(\mathbf{x})$ of the form

$$u_i(\mathbf{x},t) = \sum_{m=1}^{M} \alpha^m_i(t) f^m(\mathbf{x}), \ \ \mathbf{x}\in\Omega \ , \tag{5}$$

where $M = N + L$ with N and L being the number of boundary and internal collocation points, respectively. In this work radial basis functions are considered because of their simplicity meaning that

$$f^m(\mathbf{x}) = f(r(\mathbf{x},\xi^m)) \ , \tag{6}$$

where $r(\mathbf{x},\xi^m)$ is the Euclidean distance from point $\mathbf{x}$ to point ξ^m. Inserting expression (5) into the volume integral of Eq. (4) and using the reciprocity principle one succeeds in transforming this integral into a boundary integral of the form

$$-\int_{\mathbf{\Omega}} \mathbf{u}^*(\mathbf{x},\xi)\rho\ddot{\mathbf{u}}(\xi,t)\mathrm{d}\Omega(\xi) = \rho\sum_{m=1}^{M}\ddot{\alpha}^m_n(t)\left[c_{ij}(\mathbf{x})\psi^m_{jn}(\mathbf{x}) + \int_\Gamma p^*_{ij}(\mathbf{x},\xi)\psi^m_{jn}(\mathbf{x})\mathbf{d}\Gamma(\xi) - \int_\Gamma u^*_{ij}(\mathbf{x},\xi)\eta^m_{jn}(\mathbf{x})\mathrm{d}\Gamma(\xi)\right] \ , \tag{7}$$

where $\psi^m_{jn}(\mathbf{x})$ is the particular solution (displacement) of the equation

$$\mathbf{L}^1_{\mathbf{x}}\boldsymbol{\psi}^m(\mathbf{x}) = f^m(\mathbf{x})\mathbf{I} \tag{8}$$

and $\eta_{jn}^m(\mathbf{x})$ is the traction field corresponding to the displacement $\psi_{jn}^m(\mathbf{x})$ with $i,j,n=1,2,3$. Discretization of the boundary Γ into a finite number of quadratic boundary elements with a total number of N nodes and writing of Eq. (4) in conjunction with (7) for all these nodes, enables one to form the matrix equation

$$[\mathbf{P}]\{\mathbf{u}\} = [\mathbf{U}]\{\mathbf{p}\} + \rho([\mathbf{P}][\mathbf{\Psi}] - [\mathbf{U}][\mathbf{H}])\{\ddot{\boldsymbol{\alpha}}\} \ , \tag{9}$$

where $[\mathbf{U}]$ and $[\mathbf{P}]$ are the elastostatic influence matrices, $\{\mathbf{u}\}$ and $\{\mathbf{p}\}$ are the boundary displacement and traction vectors, respectively and $[\mathbf{\Psi}]$ and $[\mathbf{H}]$ are matrices containing submatrices of the type $\boldsymbol{\psi}_j^m$ and $\boldsymbol{\eta}_j^m$ each column of which corresponds to the m-order radial function and each row to the j nodal point. Application of expansion (5) to all nodal points M and collection of the resulting equations produces

$$\{\mathbf{u}\} = [\mathbf{F}]\{\boldsymbol{\alpha}\} \ . \tag{10}$$

Thus one can rewrite Eq. (9) into the form

$$[\mathbf{M}]\{\ddot{\mathbf{u}}\} + [\mathbf{P}]\{\mathbf{u}\} = [\mathbf{U}]\{\mathbf{p}\} \ , \tag{11}$$

where

$$[\mathbf{M}] = \rho([\mathbf{U}][\mathbf{H}] - [\mathbf{P}][\mathbf{\Psi}])[\mathbf{F}]^{-1} \ . \tag{12}$$

Equation (11) can be easily solved by a step-by-step time integration algorithm. It has been found by Loeffler and Mansur (1987) that among four different time integration algorithms (two central difference, Newmark's and Houbolt's) Houbolt's algorithm is the most accurate and stable for solving this equation. In this work, besides Houbolt's algorithm, the stiffly stable algorithm of Park (Park 1975; Adeli et al. 1978) the α-method of Hilber et al. (1977), as well as the central difference algorithm and those of Newmark and Wilson (Bathe 1996) have also been used and tested.

The corresponding DR/BEM elastodynamic formulation in frequency domain can be easily accomplished by considering time harmonic dependence for the boundary displacement and traction vectors appearing in (11). In this case Eq. (11) becomes

$$(-\omega^2[\mathbf{M}] + [\mathbf{P}])\{\mathbf{u_0}\} = [\mathbf{U}]\{\mathbf{p_0}\} \ , \tag{13}$$

where ω is the circular frequency of the harmonic excitation of $\mathbf{u}$ and $\mathbf{p}$ vectors with amplitudes $\mathbf{u}_0$ and $\mathbf{p}_0$, respectively. For any desirable frequency, by considering the appropriate boundary conditions, one can compute any unknown amplitude by solving the system (13). The computation of natural modes and frequencies of vibration can be deduced from the general system (13) by setting the external disturbances equal to zero. This results to a generalized algebraic eigenvalue problem represented by the equation

$$[\mathbf{A}]\{\mathbf{x}\} = \omega^2[\mathbf{M}^*]\{\mathbf{x}\} \ , \tag{14}$$

where matrix $[\mathbf{A}]$ is the BEM influence matrix referring to all unknown boundary variables contained in $\{\mathbf{x}\}$ and matrix $[\mathbf{M}^*]$ is obtained from $[\mathbf{M}]$ by putting zeros in its sub-columns related to specified displacements (fixed boundaries). The algebraic system (14) is solved for the natural frequencies ω and the corresponding modal shapes contained in $\{\mathbf{x}\}$. It should be noticed that matrices $[\mathbf{A}]$ and $[\mathbf{M}^*]$ are both fully populated and non symmetric and care should be taken in the choice of the appropriate eigenvalue solution algorithm. In the present work, an algorithm based on iterative similarity transformations for eigenvalue extraction of non symmetric matrices described in Press et al. (1994) was used successfully.

3
Derivation of particular solutions

In this section a general method for analytically obtaining a particular solution of Eq. (8) under three-dimensional conditions is described. This method uses Papkovich potentials instead of the Galerkin vector employed by Coleman et al. (1991) and requires the solution of lower order ordinary differential equations.

A solution of Eq. (8) in three dimensions admits (Brand 1966) a dyadic decomposition of the form

$$\boldsymbol{\psi}^m = \mathbf{a}_1 \otimes \hat{\mathbf{x}}_1 + \mathbf{a}_2 \otimes \hat{\mathbf{x}}_2 + \mathbf{a}_3 \otimes \hat{\mathbf{x}}_3 \ , \tag{15}$$

where $\otimes$ denotes the dyadic, $\mathbf{a}_i$ are unknown vectors and $\hat{\mathbf{x}}_i$ the unit vectors along x_i axes of a three dimensional Cartesian system $(i=1,2,3)$. Inserting Eq. (15) into Eq. (8) one receives

$$\sum_{i=1}^{3}[\mu\Delta\mathbf{a}_i + (\lambda+\mu)\nabla\nabla\cdot\mathbf{a}_i - f(r)\hat{\mathbf{x}}_i]\otimes\hat{\mathbf{x}}_i = \mathbf{0} \ . \tag{16}$$

Due to the orthogonality of $\hat{\mathbf{x}}_i$ Eq. (16) implies that

$$\Delta\mathbf{a}_i + \frac{1}{1-2v}\nabla\nabla\cdot\mathbf{a}_i - \frac{1}{\mu}f(r)\hat{\mathbf{x}}_i = \mathbf{0}, \ i=1,2,3 \ , \tag{17}$$

where v is the Poisson's ratio. The solutions of Eq. (17) can be expressed in terms of the vector and scalar (Rekach 1979) potentials as

$$\mathbf{a}_i = \mathbf{A}_i - \frac{1}{4(1-v)}\nabla(\mathbf{r}\cdot\mathbf{A}_i + \alpha_i), \ i=1,2,3 \ , \tag{18}$$

where the vector potentials $\mathbf{A}_i$ and the scalar potentials α_i satisfy the equations

$$\mu\Delta\mathbf{A}_i = f(r)\hat{\mathbf{x}}_i \tag{19}$$

and

$$\mu\Delta\alpha_i = -f(r)(\hat{\mathbf{r}}\cdot\hat{\mathbf{x}}_i) \ . \tag{20}$$

It is easy to see that the complete solutions of the above vector and scalar Poisson's equations (19) and (20) respectively, are

$$\mu\mathbf{A}_i = \left[g(r) + \frac{R_1}{r}\right]\hat{\mathbf{x}}_i + \frac{R_2}{r}(\hat{\mathbf{x}}_1 + \hat{\mathbf{x}}_2 + \hat{\mathbf{x}}_3 - \hat{\mathbf{x}}_i) \ , \tag{21}$$

$$\mu\alpha_i = \left[q(r) + R_3 r + \frac{R_4}{r^2}\right](\hat{\mathbf{r}}\cdot\hat{\mathbf{x}}_i) \ , \tag{22}$$

where the radial functions $g(r)$ and $q(r)$ satisfy the ordinary differential equations

$$\frac{1}{r}\frac{\mathrm{d}}{\mathrm{d}r}\left(\frac{\mathrm{d}}{\mathrm{d}r}[r\,g(r)]\right) = f(r) \ , \tag{23}$$

$$\frac{\mathrm{d}}{\mathrm{d}r}\left[\frac{1}{r^2}\frac{\mathrm{d}}{\mathrm{d}r}\{r^2 q(r)\}\right] = -rf(r) \ , \tag{24}$$

respectively, and the constants R_1, R_2, R_3, R_4 appearing in (21) and (22) correspond to arbitrary integration constants of the homogeneous solutions of (23) and (24), respectively.

Taking into account Eq. (21), (22) and inserting (18) into (15) the complete particular solution of (8) is written as

$$\psi_{ij}^m = P_1(r)\delta_{ij} + r^2 P_2(r) r_{,i}\, r_{,j} \ , \tag{25}$$

where

$$\begin{aligned} P_1(r) &= \frac{3-4\nu}{4(1-\nu)\mu}\left(g + \frac{R_1}{r}\right) \\ &- \frac{1}{4(1-\nu)\mu}\left(\frac{q}{r} + R_3 + \frac{R_4}{r^3}\right) \ , \\ P_2(r) &= -\frac{1}{4(1-\nu)\mu}\left(\frac{1}{r}\frac{\mathrm{d}g}{\mathrm{d}r} - \frac{R_1}{r^3} + \frac{1}{r^2}\frac{\mathrm{d}q}{\mathrm{d}r}\right. \\ &\left. - \frac{q}{r^3} - \frac{3R_4}{r^5}\right) \ . \end{aligned} \tag{26}$$

In (26) the constants R_1, R_2, R_3, R_4 are usually employed in order to regularize singular terms appearing in the final expressions for $g(r)$ and $q(r)$. Finally the traction field η_{ij}^m corresponding to ψ_{ij}^m is given by

$$\begin{aligned} \eta_{ij}^m &= Q_1(r)(r_{,i}\, n_j + r_{,k}\, n_k \delta_{ij}) \\ &+ Q_2(r) r_{,k}\, n_k r_{,i}\, r_{,j} + Q_3(r) n_i r_{,j} \ , \end{aligned} \tag{27}$$

with $Q_1(r), Q_2(r), Q_3(r)$ being

$$\begin{aligned} Q_1(r) &= \frac{1-2\nu}{2(1-\nu)}\left(\frac{\mathrm{d}g}{\mathrm{d}r} - \frac{R_1}{r^2}\right) \\ &- \frac{1}{2(1-\nu)}\left(\frac{1}{r}\frac{\mathrm{d}q}{\mathrm{d}r} - \frac{q}{r^2} - \frac{3R_4}{r^4}\right) \ , \\ Q_2(r) &= \frac{1}{2(1-\nu)}\left(3\frac{\mathrm{d}g}{\mathrm{d}r} - \frac{3R_1}{r^2} + \frac{5}{r}\frac{\mathrm{d}q}{\mathrm{d}r} - \frac{5q}{r^2} - \frac{15R_4}{r^4}\right) \ , \\ Q_3(r) &= -\frac{1-2\nu}{2(1-\nu)}\left(\frac{\mathrm{d}g}{\mathrm{d}r} - \frac{R_1}{r^2}\right) \\ &- \frac{1}{2(1-\nu)}\left(\frac{1}{r}\frac{\mathrm{d}q}{\mathrm{d}r} - \frac{q}{r^2} - \frac{3R_4}{r^4}\right) \ . \end{aligned} \tag{28}$$

In (25) and (27) commas represent spatial derivatives.

It was found in Agnantiaris et al. (1996), that the radial basis function $f(r) = 1 + r$ when used in the above formulation for plane elastic problems provides the best results. Thus, for this function one can find particular solutions of Eq. (8) following the procedure described above. The calculated expressions for the $\psi_{jn}^m(x)$ particular solution and its corresponding $\eta_{jn}^m(x)$ are

$$\begin{aligned} \psi_{ij}^m &= \frac{1}{4\mu(1-\nu)}\left[(3-4\nu)\left(\frac{r^2}{6} + \frac{r^3}{12}\right) + \frac{r^2}{10} + \frac{r^3}{18}\right]\delta_{ij} \\ &- \frac{1}{4\mu(1-\nu)}\left(\frac{2}{15} + \frac{r}{12}\right) r_i r_j \ , \end{aligned} \tag{29}$$

$$\begin{aligned} \eta_{ij}^m &= \frac{1}{2(1-\nu)}\left[(1-2\nu)\left(\frac{1}{3} + \frac{r}{4}\right) + \frac{1}{5} + \frac{r}{6}\right](r_i n_j + r_k n_k \delta_{ij}) \\ &- \frac{1}{2(1-\nu)}\left[(1-2\nu)\left(\frac{1}{3} + \frac{r}{4}\right) - \frac{1}{5} - \frac{r}{6}\right] r_j n_i \\ &- \frac{1}{2(1-\nu)}\left(\frac{1}{12r}\right) r_i r_j r_k n_k \ , \end{aligned} \tag{30}$$

where μ is the shear modulus, ν the Poisson's ratio, r_i and n_i are the components of the vector r connecting any two points of the boundary surface and the components of the normal outward vector n at the point where the particular solution is evaluated, respectively and δ_{ij} is the Dirac function. The indices i and j vary from 1 to 3.

4
Numerical examples

In this section two 3-D elastodynamic problems dealing with the free and forced vibration of an elastic sphere of radius $r = 6\,\mathrm{m}$ and a cube of side $\alpha = 6\,\mathrm{m}$, are solved by the DR/BEM in order to examine the efficiency and the accuracy of this method as applied to structural vibration analysis. The above applications were accomplished in a 486 personal computer with 100 MHz processor speed, 16 Mb RAM and 600 Mb hard disk memory space. The material properties for both problems are: Shear modulus $\mu = 10^6$ Pa, Poisson's ratio $\nu = 0.25$ (in the free vibration analysis of the cantilever elastic cube the Poisson's ratio is taken equal to 0.3) and mass density $\rho = 100\,\mathrm{kg/m^3}$. All the results are compared with those obtained by other analytical and/or numerical methods.

Example 1 The first problem in this example concerns the free vibration of an elastic sphere with a traction free surface. The first six natural frequencies of the problem have been calculated through the DR/BEM by discretizing the surface of the sphere into 40 continuous, nine node, quadratic, quadrilateral elements and using in turn 7, 15, 27, 53 and 67 uniformly distributed internal collocation points. The results are presented in Table 1 and compared with those derived analytically in Eringen and Suhubi (1975). As it is evident from this table there is a very good agreement between numerical and analytical results, especially when the number of internal collocation points increases. Increasing the number of internal collocation points makes the error smaller and of similar size for all the frequencies.

The same sphere is subjected next to a uniform harmonic pressure of amplitude $P_0 = 100$ Pa. This time harmonic vibration problem has been solved numerically by the DR/BEM using the same boundary mesh and the same number of internal points as in the previous free vibration problem. Figure 1a–d portrays the amplitude of the harmonic radial displacement U_r at the surface of the sphere versus the frequency ω for 0, 15, 47 and 67 internal points. The results are compared with the analytical solution of Eringen and Suhubi (1975) and those obtained by a conventional frequency domain BEM (FD/BEM) code (Kattis et al. 1994) using the same boundary mesh. It is obvious from this comparison that the accuracy of the DR/BEM increases as the number of internal points increases.

Table 1. Normalized eigenfrequencies of the traction free sphere

$\omega^* = \omega \times R \times \sqrt{\rho/\mu}$

Mode	Type	Analytical	DR/BEM 7 I.P.	Error (%)	DR/BEM 15 I.P.	Error (%)	DR/BEM 27 I.P.	Error (%)	DR/BEM 53 I.P.	Error (%)	DR/BEM 67 I.P.	Error (%)
1	Torsional	2.501	2.446	2.3	2.453	1.9	2.456	1.8	2.469	1.47	2.464	1.47
2	Spheroidal	2.640	2.873	8.8	2.777	5.18	2.750	4.1	2.691	1.93	2.691	1.93
3	Spheroidal	3.424	3.440	0.46	3.405	0.5	3.397	0.78	3.395	0.84	3.383	1.19
4	Torsional	3.865	3.883	0.45	3.881	0.4	3.877	0.3	3.874	0.23	3.873	0.23
5	Spheroidal	3.916	3.898	0.45	3.898	0.45	3.891	0.63	3.886	0.76	3.886	0.76
6	Spheroidal	4.440	4.681	5.4	4.607	3.76	4.575	3.	4.509	1.55	4.509	1.55

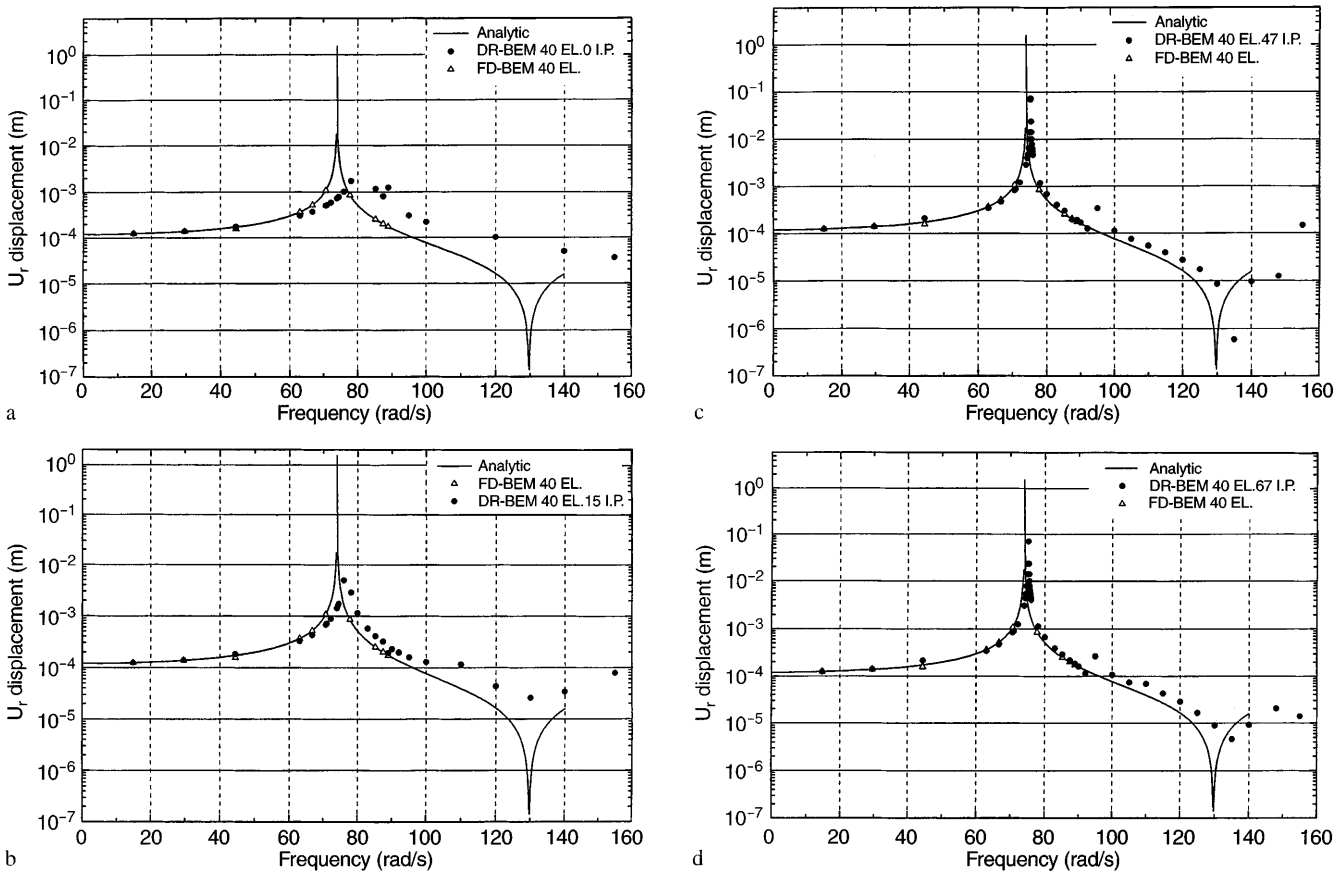

Fig. 1a–d. Amplitude of the radial displacement on the surface of the sphere versus radial frequency

Finally the sphere is subjected to a suddenly applied uniform radial pressure $P(t) = P_0 H(t)$ where $P_0 = 100$ Pa and $H(t)$ is the Heaviside function. This problem has been solved by the DR/BEM using the same mesh as in the previous two cases and considering 0, 15, 27, 53 and 67 internal collocation points. In order to find the most reliable time marching scheme of solving the final system (11), the well known step-by-step time integration techniques of Houbolt, Newmark, Wilson, central difference (Bathe 1996; Park 1975) and the α-method of Hilber et al. (1977), have been tested in the present example. Among them, only Houbolt's and Park's methods gave stable and accurate results. For this reason, only results pertaining to Houbolt's and Park's algorithms are presented here as shown in Fig. 2a–d and 3a–d, respectively, for 0, 15, 53 and 67 internal collocation points for Houbolt's and 0, 15, 27 and 53 for Park's methods. In both cases the same time integration step $\Delta t = 0.0038$ sec has been used for comparison reasons. The results are compared with those obtained first by a numerical inverse Fourier transformation (with 50 sampling points in a time interval of 0.4 sec) of the frequency domain analytical solution given by Eringen and Suhubi (1975) and second by inverting in real time the Laplace transformed BEM solution of the problem (with 70 sampling points in a time interval of 0.6 sec) as proposed by Stamos and Beskos (1995). As it is evident from these two figures, the accuracy of the DR/BEM solution through both Houbolt's and Park's step-by-step integration schemes, slightly increases for a small increase of the number of internal points but decreases for further increase of them. In fact, Park's algorithm breaks down when use is made of 53 internal points (Fig. 3d). This is in

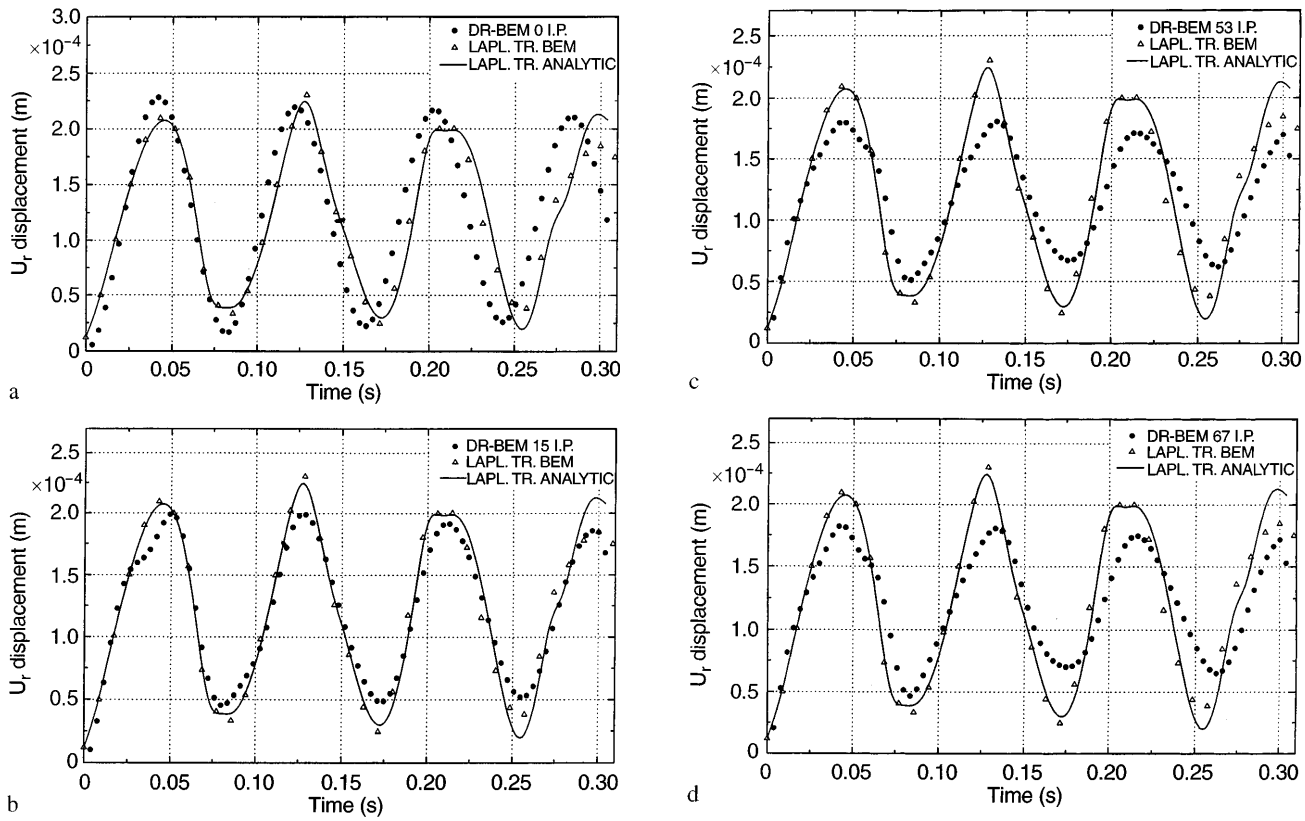

Fig. 2a–d. Time history of the radial displacement on the surface of the sphere using Houbolt's algorithm

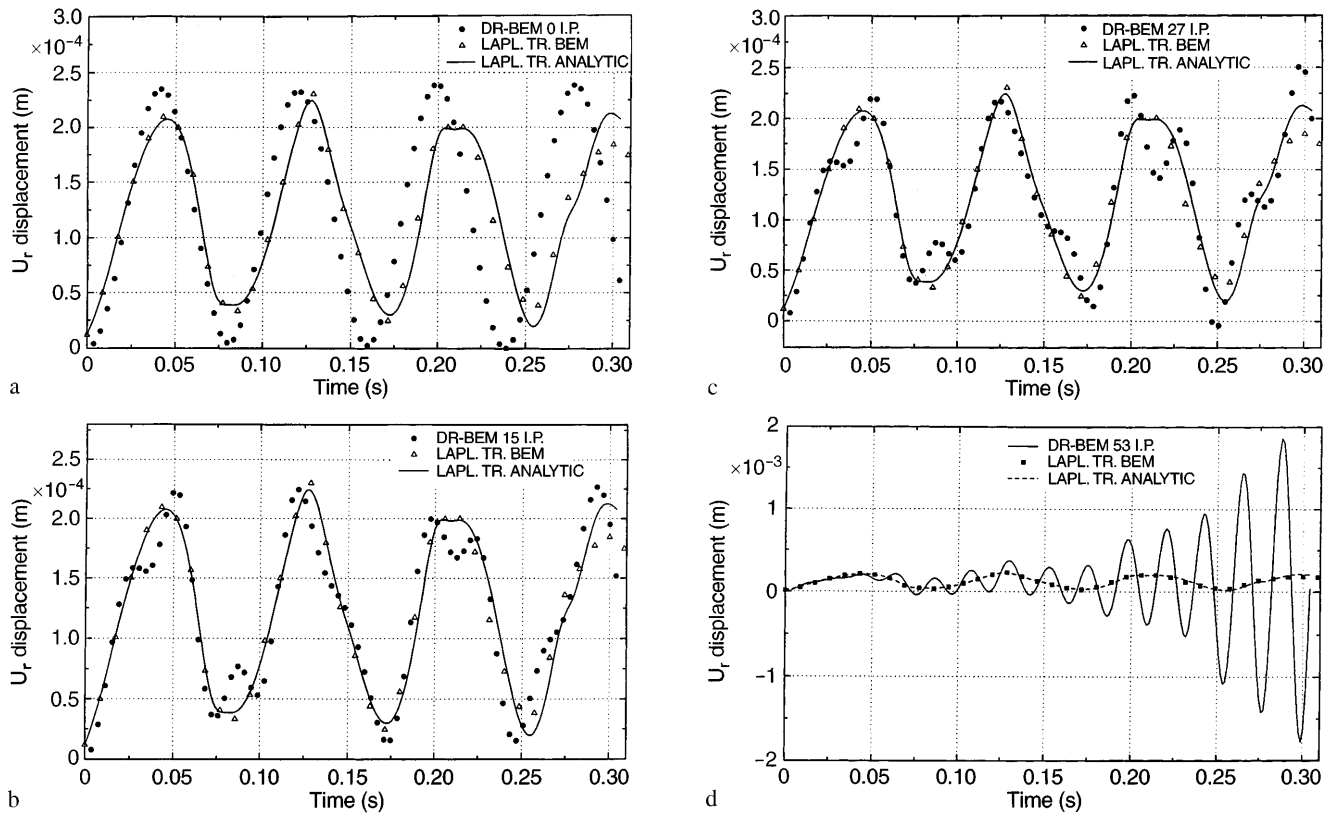

Fig. 3a–d. Time history of the radial displacement on the surface of the sphere using Park's algorithm

Table 2. Normalized eigenfrequencies of the cantilever cube

$\omega^* = \omega \times R \times \sqrt{\rho/E}$

Mode	Type	Analytical	DR/BEM 0 I.P.	Error (%)	DR/BEM 10 I.P.	Error (%)	DR/BEM 27 I.P.	Error (%)	DR/BEM 36 I.P.	Error (%)
1	Bending	0.670	0.673	0.44	0.670	0.	0.670	0.	0.670	0.
2	Torsion	0.909	0.926	1.83	0.930	2.3	0.933	2.64	0.933	2.64
3	Tension	1.599	1.628	1.81	1.608	0.5	1.602	0.18	1.6	0.06
4	Bending	1.769	1.788	1.07	1.775	0.3	1.773	0.22	1.773	0.22
5	Torsion	2.180	2.149	2.6	2.154	1.2	2.156	1.1	2.156	1.1
6	Tension	2.581	2.533	1.85	2.559	0.8	2.556	0.96	2.557	0.92

agreement with Chirino et al. (1994) and Agnantiaris et al. (1996) stating that a small number of internal points improves the accuracy of the solution.

It should be noted here that both Houbolt's and Park's algorithms have been also tested in the present example by considering either smaller or larger time step than the one used here (0.0038 sec) for the same number of internal collocation points. These results are not shown here for lack of space reasons, but the main conclusion of this study is that Houbolt's integration scheme gives accurate results for a time step Δt that satisfies the relation $\beta = c_1 \Delta t / L = 0.8$, with c_1 and L being the longitudinal wave velocity of the elastic medium and the length between the nearest surface nodes, respectively, while Park's stiffly stable time integration scheme works with the same accuracy as Houbolt's algorithm when β is equal to 1.4. For 2-D applications of the DR/BEM this parameter β takes values in the interval [0.75, 1.5] when Houbolt's integration technique is used (Chirino et al. 1994).

Example 2 The first problem in this example deals with the free vibration analysis of an elastic cube. The displacements on one face of the cube are completely fixed while all the other faces are traction free. The cube is discretized into 4 nine-node-quadratic-quadrilateral discontinuous elements per face in order to accommodate the

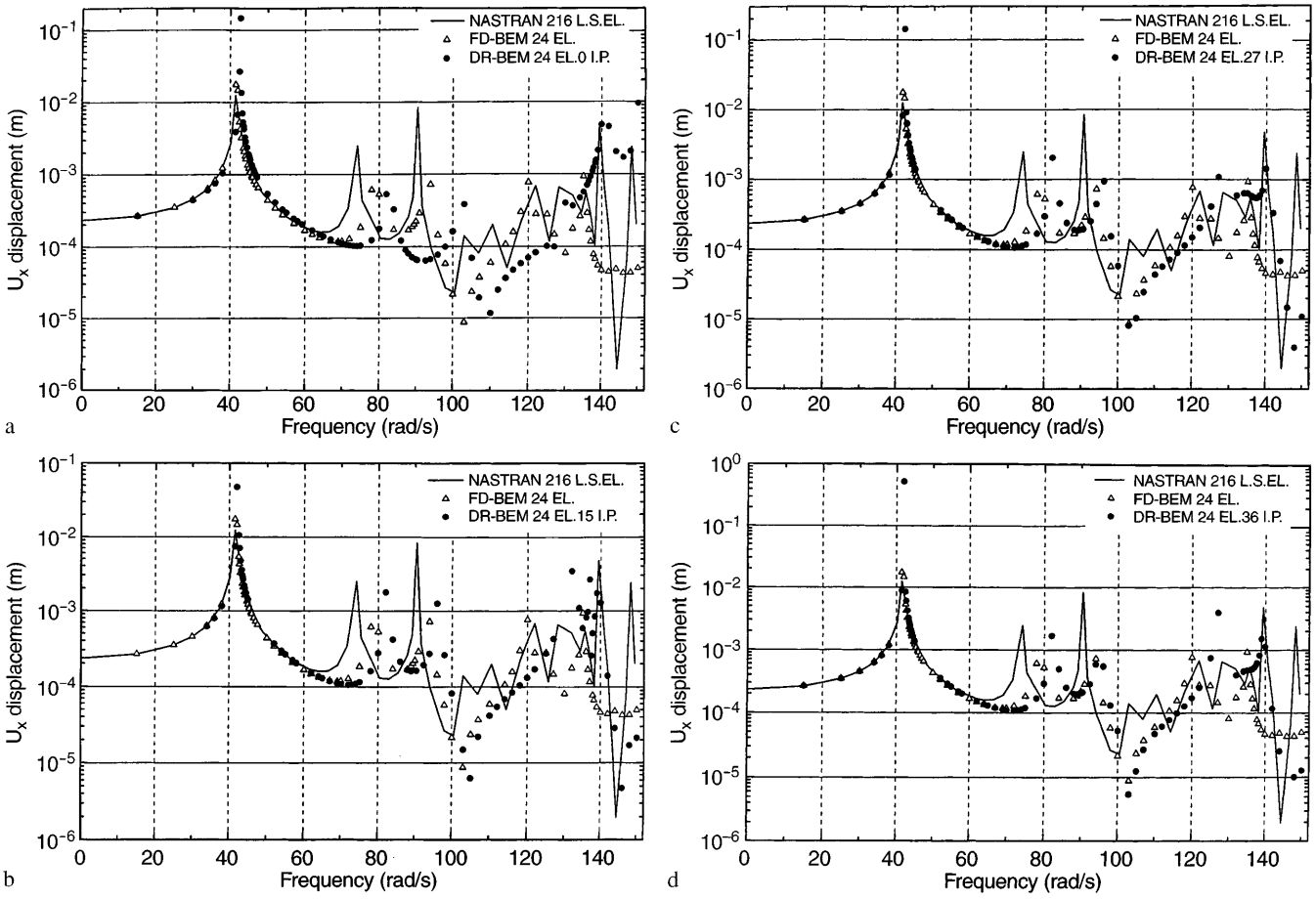

Fig. 4a–d. Amplitude of the U_x displacement at the mid-node of the loaded surface of the cube versus radial frequency

corner and edge effects. The results of the DR/BEM were obtained with 0, 10, 27 and 36 internal collocation points. The first six natural frequencies of the structure as obtained by the DR/BEM are shown in Table 2. The results show a rapid convergence as the number of internal points increases and are in excellent agreement with those calculated analytically by Leissa and Zhang (1983).

Next, a harmonic forced vibration problem is considered. The cube is subjected to a uniform harmonically varying with time normal tensile traction of amplitude $P_0 = 100$ Pa acting on one face (along x direction), while the displacements on the opposite face are completely fixed. The remaining faces are traction free. The boundary mesh is the same as in the free vibration case. The amplitude of the harmonic displacement U_x on the loaded face is plotted versus frequency ω as shown in Figs. 4a–d for 0, 15, 27 and 36 internal collocation points. The same problem was also solved by the finite element program NASTRAN (1994) using 216 solid-linear-finite-elements as well as by a conventional frequency domain BEM (FD/BEM) code (Kattis et al. 1994) using the same surface mesh as in the DR/BEM. The results of the DR/BEM are shown to be in close agreement with those obtained by NASTRAN and in closer agreement with those obtained by the frequency domain BEM, especially when more internal collocation points are included.

Finally the cube is subjected at one of its faces to a suddenly applied uniform tensile traction $P = P_0 H(t)$ acting along the x direction, where $P_0 = 100$ Pa and $H(t)$ is the Heaviside function. The boundary mesh used consists again of 4 elements per face. The time step used in Houbolt's time integration scheme is $\Delta t = 0.0075$ sec $(\beta = 0.8)$ while in Park's stiffly stable scheme is $\Delta t = 0.0128$ sec $(\beta = 1.4)$. The results of the DR/BEM were obtained with 0, 3, 10 and 27 internal collocation points. The time history of the U_x displacement at the middle node of the loaded surface of the cube is compared with that obtained by the finite element program NASTRAN using 216 solid-linear-finite-elements and the Newmark-linear-acceleration time integration algorithm with a time step $\Delta t = 0.0032$ sec. The transient displacement response is shown in Figs. 5a–d for both the Houbolt's and Park's algorithms. The results are in good agreement with those obtained by NASTRAN but, as it is evident from the graphs, inclusion of internal collocation points here introduces oscillations in the response obtained by both Houbolt's and Park's schemes in agreement with the results of the previous example. As a matter of fact, in here, even a small number of interior points does not improve the accuracy as in the case of 2-D plastodynamics analysed by the DR/BEM (Kontoni and Beskos 1993). Also one can observe that the responses calculated by the DR/BEM are stiffer than those obtained by NASTRAN probably to the higher numerical damping in Houbolt's and Park's algorithms as compared to the Newmark's algorithm employed by NASTRAN.

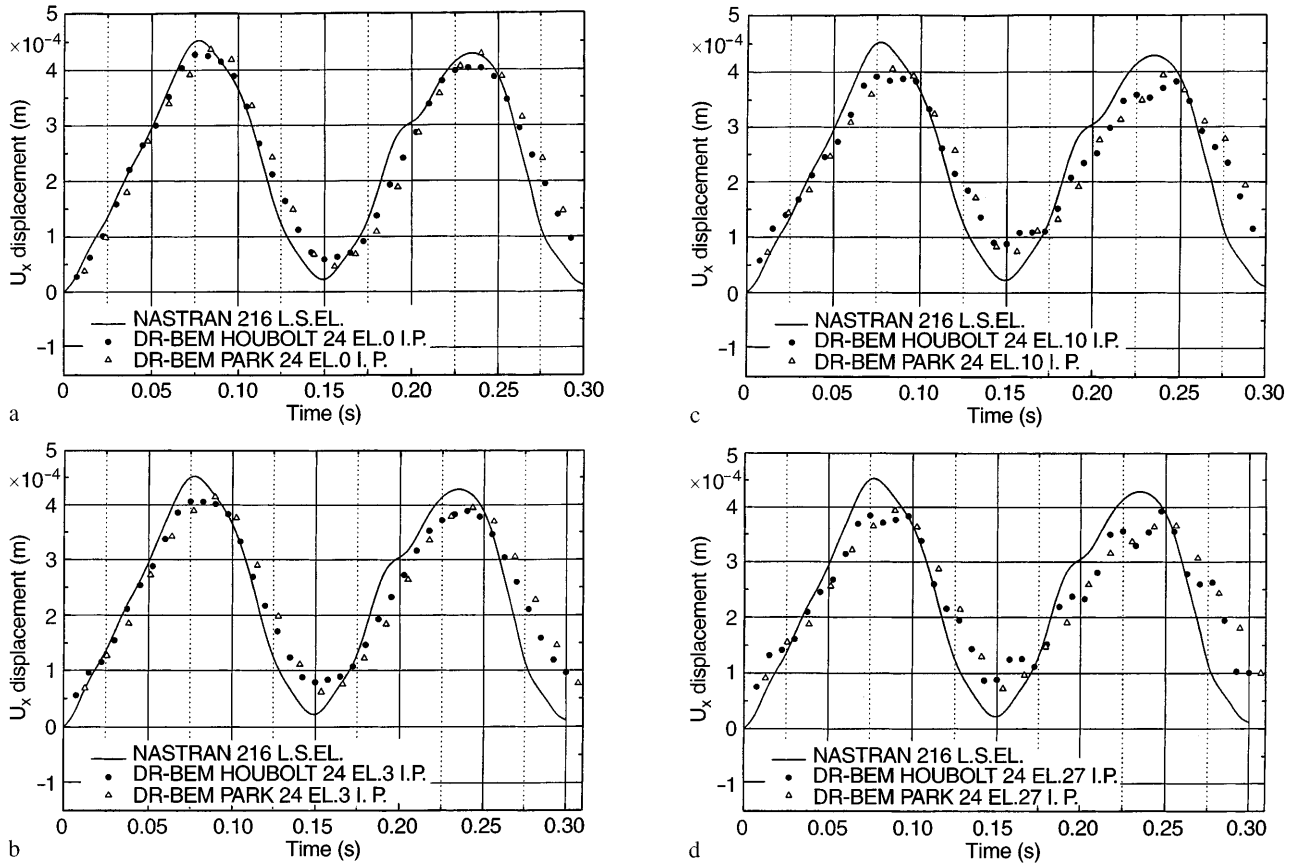

Fig. 5a–d. Time History of the U_x displacement at the mid-node of the loaded surface of the cube

On the basis of the above two examples one can observe that, in general, an increase of the number of interior points increases the accuracy of the results of free vibration or harmonic forced vibration analyses, while decreases the accuracy of the results of transient forced vibration analysis, unless this increase of the interior points is small. These results can be attributed to the fact that increase of internal points increases the number of degrees of freedom of the structure and this results to a higher solution accuracy when one computes the first few vibration modes or the harmonic response for low frequencies and a lower solution accuracy when one computes the transient response taking into account the effect of many inaccurately computed higher modes.

A comparison of the present 3-D elastodynamic results against the 2-D ones of Agnantiaris et al. (1996) clearly indicates that the DR/BEM is more accurate and efficient when used for 2-D than for 3-D problems.

5 Conclusions

An efficient and satisfactorily accurate DR/BEM for 3-D dynamic analysis including both free and forced vibrations has been developed. Closed form expressions for the particular solution of displacement and traction tensors are provided for the case of radial basis functions. Only the surface of the structure has to be discretized eventhough in eigenfrequency and harmonic response analyses, internal collocation points are necessary for increased accuracy. In harmonic response problems the 3-D DR/BEM provides excellent results especially for low frequencies. The 3-D DR/BEM, like the 2-D one, produces accurate results provided that the elements over the surface of the structure are as uniformly distributed as possible.

For transient response problems, among the various step-by-step time integration schemes (Houbolt, Park, Newmark, central difference, Wilson, α-method) that can be used in DR/BEM, Houbolt's and Park's algorithms give the most accurate results with the former being slightly better. Inclusion of zero or a few internal collocation points in DR/BEM used in solving 3-D transient response problems improves the solution accuracy. However, inclusion of many interior points decreases the solution accuracy, especially when the time interval for both the Houbolt and Park schemes is small, that is when the parameter β is smaller than 0.8 for Houbolt's and 1.4 for Park's algorithms. The 3-D DR/BEM requires less computer time than the conventional time and frequency domain BEM formulations but also has large requirements on available computer memory and on available hard disk memory space due to the cumbersome matrix manipulations for the determination of the mass matrix $[\mathbf{M}]$.

References

Adeli H, Gere JM, Weaver W Jr (1978) Algorithms for nonlinear structural dynamics. Journal of Struct. Div. ASCE 104:263–280

Agnantiaris JP, Polyzos D, Beskos DE (1996) Some studies on Dual Reciprocity BEM for elastodynamic analysis. Comput. Mech. 17:270–277

Ahmad S, Banerjee PK (1986) Free vibration analysis by BEM using particular integrals. J. Eng. Mech. ASCE 112:682–695

Bathe KJ (1996) Finite Element Procedures. Prentice-Hall, Englewood Cliffs, New Jersey

Beskos DE (1987) Boundary element methods in dynamic analysis. Appl. Mech. Rev. 40:1–23

Beskos DE (1996) Boundary element methods in dynamic analysis: Part II (1986–1996). Appl. Mech. Rev. (to appear)

Brand L (1966) Vector and Tensor Analysis. John Wiley & Sons, London

Chirino F, Gallego R, Saez A, Dominguez J (1994) A comparative study of three boundary element approaches to transient dynamic crack problems. Eng. Anal. with Boundary Elem. 13:11–19

Coleman CI, Tullock DL, Phan-Thien N (1991) An effective boundary element method for inhomogeneous partial differential equations. J. Appl. Math. Phys. (ZAMP) 42:730–745

Dominguez J (1993) Boundary Elements in Dynamics. Computational Mechanics Publications and London: Elsevier Applied Science, Southampton

Eringen C, Suhubi ES (1975) Elastodynamics, Vol. II: Linear Theory. Academic Press, New York

Hilber HM, Hughes TJR, Taylor RL (1977) Improved numerical dissipation for time integration algorithms in structural dynamics. Earthquake Eng. Struc. Dyn. 5:283–292

Kattis SE, Polyzos D, Beskos DE (1994) Dynamic response analysis of 3-D elastic systems by an improved frequency domain BEM. In: Brebbia CA (ed) Boundary Element Method XVI, pp. 521–528. Computational Mechanics Publications, Southampton, Boston

Kontoni PDN, Beskos DE (1993) Transient dynamic elastoplastic analysis by the dual reciprocity BEM. Eng. Anal. with Boundary Elem. 12:1–16

Leissa A, Zhang Z (1983) Three-dimensional vibrations of the cantilever rectangular parallelepiped. J. Acoust. Soc. Am. 73:2013–2021

Loeffler CF, Mansur WJ (1987) Analysis of time integration schemes for boundary element applications to transient wave propagation problems. In: Brebbia CA, Venturini WS (eds) Boundary Element Techniques: Applications in Stress Analysis and Heat Transfer, pp. 105–122. Computational Mechanics Publications, Southampton

MSC/NASTRAN (1994) Reference Manual. The Mac-Neal-Schwendler Corporation, Los Angeles

Nardini D, Brebbia CA (1982) A new approach to free vibration analysis using boundary elements. In: Brebbia CA (ed) Boundary Element Methods in Engineering, pp. 313–326. Springer, Berlin

Nardini D, Brebbia CA (1983) Transient dynamic analysis by the boundary element method. In: Brebbia CA, Futagami T, Tanaka M (eds) Boundary Elements, pp. 719–730. Springer, Berlin

Nardini D, Brebbia CA (1985) Boundary integral formulation of mass matrices for dynamic analysis. In: Brebbia CA (ed) Topics in Boundary Element Research, Vol. 2: Time-Dependent and Vibration Problems, pp. 191–208. Springer, Berlin

Park KC (1975) An improved stiffly stable method for direct integration of nonlinear structural dynamic equations. J. Appl. Mech. (ASME). 42:464–470

Polyzos D, Dassios G, Beskos DE (1994) On the equivalence of dual reciprocity and particular integrals approaches in the BEM. Boundary Elem. Commun. 5:285–288

Press WH, Teukolsky SA, Vetterling WT, Flannery BP (1994) Numerical Recipes in FORTRAN, The Art of Scientific Computing, 2nd edn. University Press, Cambridge

Providakis CP, Beskos DE, Sotiropoulos DA (1994) Dynamic analysis of inelastic plate by the D/BEM, Comput. Mech. 13:276–284

Rekach VG (1979) Manual of the Theory of Elasticity. Mir Publishers, Moscow

Stamos AA, Beskos DE (1995) Dynamic analysis of large 3-D underground structures by the BEM. Earthquake Eng. Struct. Dyn. 24:917–934
Wang HC, Banerjee PK (1988) Axisymmetric free-vibration problems by the boundary element method. J. Appl. Mech. (ASME) 55:437–442
Wang HC, Banerjee PK (1990) Free vibration of axisymmetric solids by BEM using particular integrals. Int. J. Numer. Meth. Eng. 29:985–1001
Wilson RB, Miller NM, Banerjee PK (1990) Free vibration analysis of three-dimensional solids by BEM. Int. J. Numer. Meth. Eng. 29:1737–1757